

Profile loss and turbulence modelling in radial outflow turbine cascades

Tomovska Elena, Grönman Aki, Turunen-Saaresti Teemu

This is a Publisher's version version of a publication
published by The European Turbomachinery Society
in 15th European Conference on Turbomachinery Fluid dynamics & Thermodynamics

DOI: 10.29008/ETC2023-106

Copyright of the original publication:

© by Author

Please cite the publication as follows:

Tomovska, E., Grönman, A., Turunen-Saaresti, T. (2023). Profile loss and turbulence modelling in radial outflow turbine cascades. In: Proceedings of the 15th European Conference on Turbomachinery Fluid dynamics & Thermodynamics. DOI: 10.29008/ETC2023-106

**This is a parallel published version of an original publication.
This version can differ from the original published article.**

PROFILE LOSS AND TURBULENCE MODELLING IN RADIAL OUTFLOW TURBINE CASCADES

E. Tomovska – A. Grönman – T. Turunen-Saaresti

Laboratory of Fluid Dynamics, LUT University, Lappeenranta, Finland, gronman@lut.fi

ABSTRACT

Radial outflow turbines (ROT) offer an alternative to single-stage high-work axial turbines, for example, in steam and organic Rankine cycle applications. Previous studies have shown that axial turbine loss correlations tend to over-predict losses in comparison with numerical data. However, only part of the most used loss correlations has so far been subjected to analysis while, additionally, the effect of turbulence modelling has not been widely covered in the open literature exploring ROTs. This study, therefore, examines the accuracy of a particular loss model known as Traupel's model on ROT profile loss prediction by comparing it with validated numerical simulations. In addition, the effects of different turbulence models on the flow fields are studied in detail. In doing so, this research shows that Traupel's model tends to over-predict loss. Crucially, the turbulence modelling approach is found to affect results significantly, which mainly originate from differences in the boundary layer and turbulence predictions.

KEYWORDS

RADIAL OUTFLOW TURBINE, PROFILE LOSS, TURBULENCE MODELLING

NOMENCLATURE

Latin alphabet

M	Mach number	[-]
p	static pressure	[Pa]
p_t	total pressure	[Pa]
Y_{Tot}	total pressure loss	[-]

Greek alphabet

ζ	loss coefficient	[-]
χ	correction factor	[-]

Subscripts

1	cascade inlet
2	cascade outlet
C	shock
M	freestream velocity
P0	basic profile
R	Reynolds number
Te	trailing edge

Abbreviations

ORC	organic Rankine cycle
RANS	Reynolds-averaged Navier–Stokes
RNG	re-normalisation group
ROT	radial outflow turbine
RS	Reynolds stress
SST	shear stress transport
BSL	baseline
SSG	Speziale, Sarkar and Gatski
TI	turbulence intensity

INTRODUCTION

Turbines featuring powers ranging from hundreds of kilowatts up to a few megawatts are used in many applications. These applications include large ships, for example, in which a small steam turbine can improve energy production efficiency by several percentage points (Lion et al. [2020], Uusitalo et al. [2019]). In addition, biomass power plants offer the opportunity to utilise turbines below a few megawatts. For these applications, a decision is usually taken on which energy conversion technology to favour: the Rankine cycle or the organic Rankine cycle (ORC). In these small-scale Rankine cycle applications, it has been suggested that a radial outflow turbine could replace single-stage high-work turbines (Leino et al. [2016]). Although radial outflow turbines have also gained attention in the context of ORC and supercritical CO₂ power cycles (Persico et al. [2013], Grönman and Uusitalo [2021]).

The increasing popularity of ROTs is at least partly explained by the good off-design performance expected, as well as their relatively small physical size when compared to impulse-type axial turbines. ROTs are capable of handling reasonably high volume flow, while the expected Mach number levels are also comparably low, as discussed by Persico et al. (2013). Plus, these turbines can reduce the need for partial admission.

Axial turbine loss correlations are typically utilised for the design of radial outflow turbines. Pini et al. (2013) and Casati et al. (2014), for example, both employed the Craig and Cox (1971) loss correlation in their studies, while the correlation of Kacker and Okapuu (1981) was used by Al Jubori et al. (2017). Grönman et al. (2020a) also presented results indicating that Soderberg's loss correlation (Dixon, 2005) performed well in ROT application. Additionally, there are a few studies that have examined the accuracy of common axial turbine loss correlations on ROTs. Both Persico et al. (2013) and Grönman et al. (2017), when conducting an examination of loss correlations, have reported a tendency of primary loss over-prediction. In Persico's study, the reason for this over-prediction was connected to differences in wake strength, which was weaker in ROTs than in axial turbines.

The turbulence modelling approach is known to have a significant effect on results but, to the authors' knowledge, these effects have not yet been studied in the context of ROTs. There are several available studies, however, that compare different turbulence models, which show that the most common approach in turbomachinery is to use the $k-\omega$ SST turbulence model. Nevertheless, depending on the modelled phenomena, different turbulence models can perform better than the alternatives, while the literature does not clearly show that the $k-\omega$ SST is always the best choice. In a study by Djouimaa et al. (2007), six turbulence models were compared in a transonic turbine cascade in 2D. The findings showed that the RNG $k-\epsilon$, Realisable $k-\epsilon$, Spalart-Allmaras and Reynolds stress model all outperformed $k-\omega$ SST in the prediction of blade isentropic Mach number. Another study by Patel et al. (2014) explored the role of turbulence models in a transonic steam turbine cascade. Their conclusions found that the $k-\omega$ and $k-\epsilon$ turbulence models did not predict the expected condensation shock at all, although other models – including $k-\omega$ SST – did manage to capture it. Regarding radial inflow turbines, Yuan et al. (2021) compared three turbulence models against measurements, finding that $k-\omega$ SST performed better than the standard $k-\omega$ or $k-\epsilon$. Whereas Liu et al. (2008) studied the effect of turbulence models on the modelling of an axial compressor tip vortex. Among the tested models, they found the Reynolds stress (RS) turbulence model to be the most effective in predicting the tip-leakage vortex, although other models such as $k-\omega$ SST and $k-\epsilon$ did also have their strengths in vortices modelling.

Based on the open literature, there is still a lack of understanding about loss correlations and turbulence modelling in radial turbines and our study performs a combined turbine loss model and CFD analysis that aims to answer the following questions:

1. How does Traupel's axial turbine loss correlation predict the primary losses in radial outflow turbines compared to numerical simulations?
2. Which RANS turbulence model should be used to model primary losses in radial outflow turbines?

The article begins with an introduction to primary loss modelling, which is followed by a presentation of the numerical approach. A grid dependency study is then presented before the results and conclusions sections.

METHODS

Primary loss modelling

A study by Zhdanov et al. (2013) compared several axial turbine loss correlations and the results showed that Traupel's model (Traupel, 1977) is capable of predicting turbine efficiency with an accuracy of $\pm 1.5\%$. This accuracy level is similar to many commonly used loss correlations. The Traupel's loss correlation predicts losses separately for primary, secondary, tip clearance, and fan losses. However, as this work focuses on primary losses, they are the only losses defined here. Traupel's primary loss coefficient is defined based on the Reynolds number effect factor χ_R , free-stream velocity correction factor χ_M , basic profile loss ζ_{P0} , trailing edge loss ζ_{Te} , and shock loss ζ_C , as follows:

$$\zeta_P = \chi_R \chi_M \zeta_{P0} + \zeta_{Te} + \zeta_C \quad (1)$$

For this study, shock loss is set to zero due to low Mach number levels. Loss comparisons with numerical simulations are made in terms of total pressure losses and the connection between Traupel's loss coefficient and total pressure loss coefficient Y_{Tot} is defined as:

$$Y_{Tot} = \zeta_P \left(1 + \frac{\gamma M_2^2}{2} \right) \quad (2)$$

Numerical modelling

This study employs a finite volume approach by using Ansys CFX 2019 R2. The grids utilised are generated by Pointwise V17.3 R5. A second-order discretisation is used in all simulations, together with a double-precision solver. Compressible air is used as fluid and simulations are run in 2D. An O-type mesh is also used with the domain presented in Fig 1 (a) and details of the grid in Fig 1 (c). Total pressure, flow angle, turbulence intensity (TI), eddy length scale, and static temperature were used as inlet boundary conditions and static pressure at the outlet boundary. The blade is modelled as a no-slip wall while periodic boundaries are used between the flow channels. Additionally, the symmetry boundary condition is applied at the top and bottom of the one-cell height domain. The boundary conditions were set to match the experimental conditions of Grönman et al. (2020b). Table 1 presents the main design parameters of the blade cascade and the conditions present during experiment. The convergence of each solution was determined when the residuals applied were below 10^{-6} and the imbalance was below 0.01%. In addition, it is also worth mentioning that all results presented in this work are mass flow averaged.

Overall, seven turbulence models were compared, while the k- ω SST model (Menter, 1993) was adopted in the grid independency study since it is a commonly used approach. The other six turbulence models were chosen to compare different turbulence models in the present application.

These models consist of one equation model of Spalart and Allmaras (Spalart, Allmaras and Johnson, 2012), two-equation models $k-\varepsilon$ (Launder and Sharma, 1974), $k-\varepsilon$ re-normalisation group (RNG) (Yakhot et al., 1992), $k-\omega$ by Wilcox (1994), and the two Reynolds stress models of baseline (BSL) and SSG (Speziale et al., 1991).

Three curved measurement planes were used, as presented in Fig. 1 (a). Plane 1 corresponds to the location of static pressure measurements taken from Grönman et al. (2020b) – see measurement plane 1 in Fig. 1 (b) as measurements 1–15. In Fig. 1 (a), planes 2 and 3 are located close to the trailing edge and are used to compare turbulence-related data in the wake area. These two planes are oriented perpendicular to the trailing edge at a constant radius. In addition, the static pressure measurements of Grönman et al. (2020b) located in the middle of the flow channel are used for later comparison. These measurement points are presented in Fig. 1 (b) as measurements 16–19. At the inlet of the test section, total pressure and turbulence intensity were measured. In addition, static temperature was measured upstream from the insulated test section.

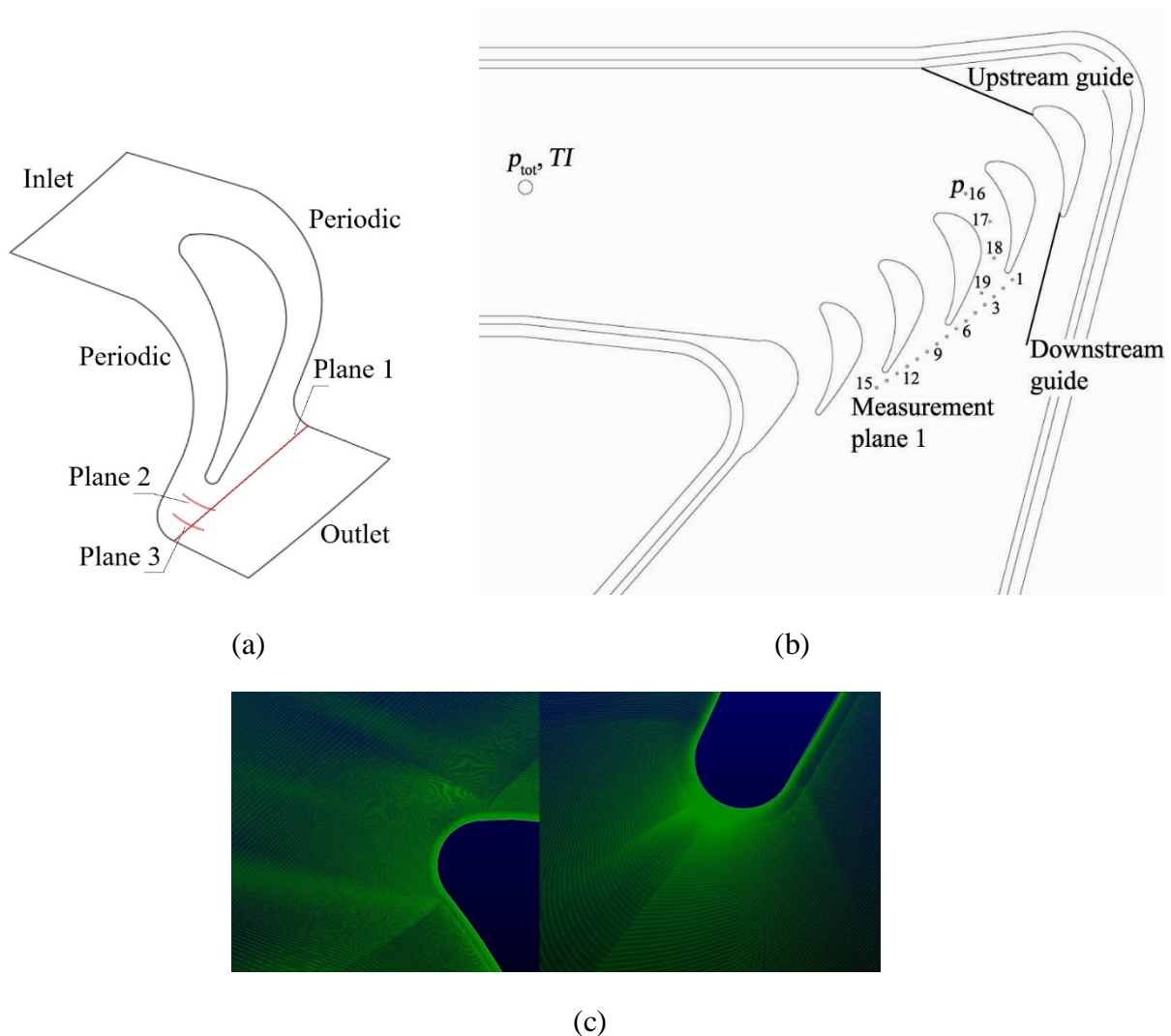


Figure 1: Schematic presentation of the numerical model domain and measurement planes (a), schematic presentation of the experimental setup by Grönman et al. (2020b) (b), and grid illustration at the leading and trailing edges (c).

Table 1: Blade operating conditions and design parameters.

Variable	Value
Isentropic Mach number	0.34
Turbulence intensity	4.3%
Chord Reynolds number	240 000
Blade inlet angle	47.5°
Blade outlet angle	67.3°
Pitch-to-chord ratio (inlet)	0.68
Pitch-to-chord ratio (outlet)	0.75

Grid dependency

For the grid dependency study, six grids were studied ranging from 266 956 cells up to 1 682 176. The analysis concentrated on total pressure loss coefficient and isentropic Mach number distribution. The pressure loss coefficient is defined as follows:

$$Y_{Tot} = \frac{P_{t1} - P_{t2}}{P_{t1} - P_2} \quad (3)$$

The analysis, as for Fig. 2 (a), shows that the total pressure loss coefficient does not change considerably (maximum change 0.16%) when the number of cells changes from 774 996 cells in Grid 4 to the higher values of Grids 5 and 6. In addition, the isentropic Mach number distribution at measurement plane 1 hardly varies at all when the grid changes (maximum variation 0.82%). Similar findings were also made for blade passage streamwise isentropic Mach number distribution (not shown here). Therefore, it was concluded that Grid 4 should be used later in this study.

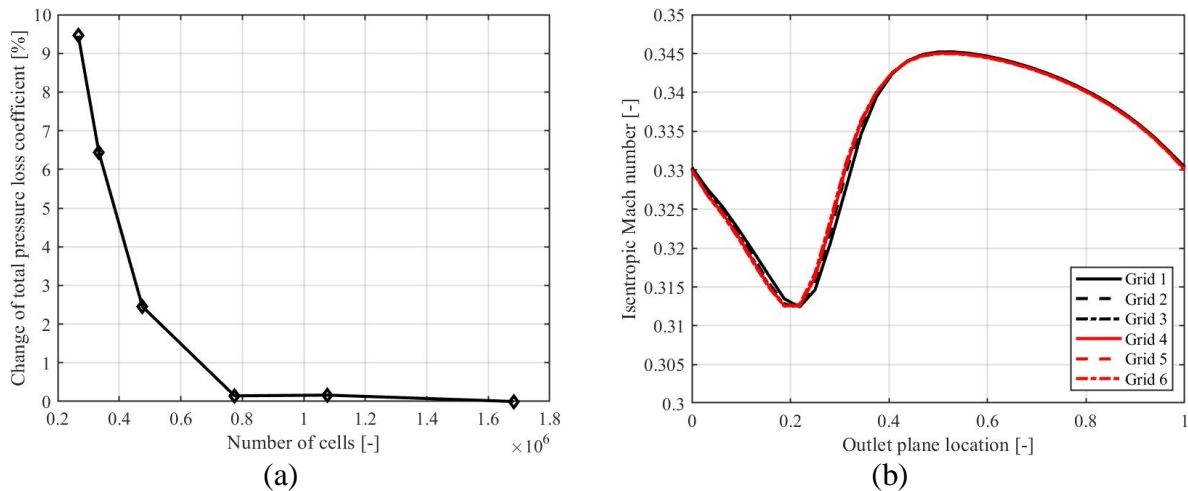


Figure 2: Effect of the number of cells on total pressure loss coefficient (a) and isentropic Mach number at measurement plane 1 (b).

RESULTS

Accuracy of turbulence models and turbine loss model

The turbulence modelling approach has a great effect on the predicted total pressure loss coefficient, as shown in Table 2. Traupel's loss model tends to over-predict primary loss more extensively than the other studied turbulence models. This finding supports previous understandings of alternative axial turbine primary loss correlations that have been applied to ROTs, as with Persico et al. (2013) and Grönman et al. (2017). From the studied turbulence model's point of view, Spalart–Allmaras is closest to Traupel, followed by $k-\omega$ and $k-\omega$ SST. Both the $k-\varepsilon$ and Reynolds stress models clearly predicted the lowest loss coefficients. The following section aims to answer the question: which models are most accurate and why?

Table 2: Comparison between the primary loss predictions of Traupel's loss model and different turbulence models. The last column shows the difference between the Traupel's loss model and turbulence models.

Loss prediction approach	Total pressure loss coefficient	Difference [%]
Traupel	0.0804	-
Spalart–Allmaras	0.0800	0.4
$k-\varepsilon$	0.0684	14.9
$k-\varepsilon$ RNG	0.0549	31.7
$k-\omega$	0.0785	2.3
$k-\omega$ SST	0.0741	7.8
BSL Reynolds stress	0.0666	17.1
SSG Reynolds stress	0.0520	35.3

Model validation and effect of turbulence modelling approach on flow characteristics

The chosen turbulence model affects the prediction of flow acceleration inside the blade flow channel, as presented in Fig. 3 (a). When compared to the experimental data, the one equation model, $k-\omega$, $k-\omega$ SST and BSL Reynolds stress models predict similar trend shapes as in the experiments. The rest of the models, however, do predict a small drop in the isentropic Mach number as the flow approaches the passage outlet (location 1 in Fig. 3). In addition, these models also differ more in general from the experimental data. Small part of the observed differences between the modelled and measured values are most likely since the experimental results were produced by a low aspect ratio cascade, in which the 3D effects can have more impact on the results. This conclusion is drawn based on an earlier study by Grönman et al. (2020b), in which a similar under-prediction trend was noticed, including with the 3D CFD.

A closer look at the pitch-wise isentropic Mach number distribution in Fig. 3 (b) reveals further differences as a result of the turbulence modelling approach. Generally speaking, all models under-predict the maximum isentropic Mach number and over-predict the minimum. The capability of each model for predicting the location of the minimum isentropic Mach number value and the wake location varies significantly. Two of the models – $k-\omega$ and $k-\omega$ SST – are capable of predicting the minimum value at the same location as the experiments. Both Reynolds stress models and the Spalart–Allmaras produce results that slightly under- or over-predict the minimum with accuracies that are nearly equal, while the $k-\varepsilon$ models are clearly mispredicting. Based on the results discussed,

comparing the measurements allows for concluding that the best-performing turbulence models are able to predict isentropic Mach number trends both inside and outside the cascade with reasonable accuracy (uncertainty of isentropic Mach number at design conditions was estimated to be ± 0.001).

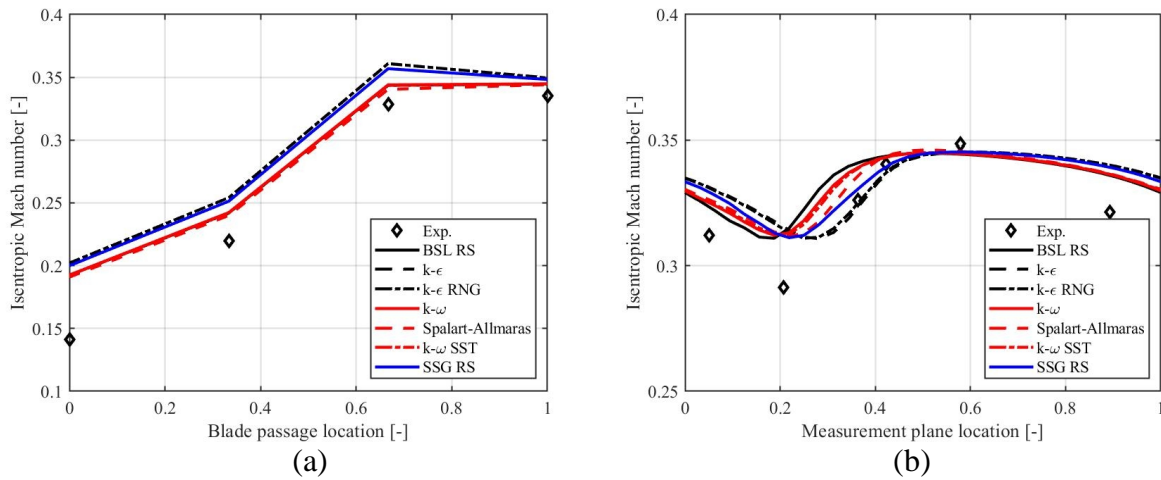


Figure 3: Effect of turbulence model on blade passage flow acceleration in the middle of the channel (a). Effect of turbulence model on blade outlet isentropic Mach number prediction (b) in measurement plane 1.

The choice of turbulence model can also have a significant effect on blade surface pressure distribution. Figure 4 contains an example of three of the models – namely, SSG Reynolds stress, $k-\epsilon$, and $k-\epsilon$ RNG – predicting a significantly larger peak value close to the trailing edge when compared to four other models. In an earlier study by Djouimaa et al. (2007), it was also observed that the $k-\epsilon$ and $k-\epsilon$ RNG models can experience surface pressure prediction challenges close to the trailing edge. These findings are likely connected with the boundary layer modelling capabilities between the different models with curved surfaces.

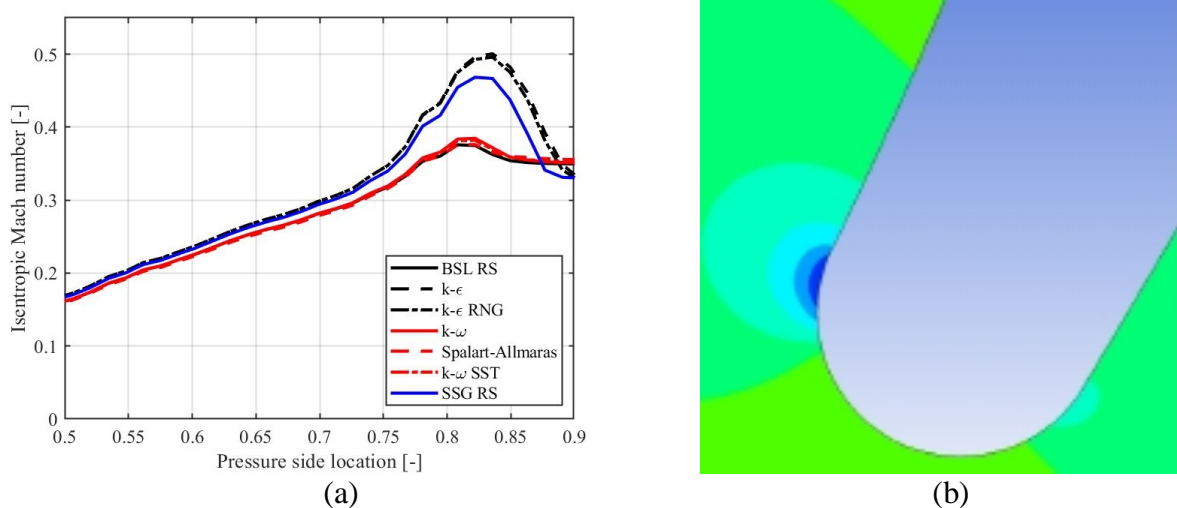


Figure 4: Effect of turbulence model on blade pressure side isentropic Mach number distribution close to trailing edge (a), and pressure contours close to trailing edge with the $k-\epsilon$ turbulence model (b).

The chosen turbulence model can also have a significant effect on turbulent kinetic energy prediction, as presented in Figs. 5 (a) and (b). It is clearly visible that $k-\omega$, $k-\omega$ SST and BSL Reynolds stress models predict profiles that are reasonably similar, with peak values arising from the blade's pressure side. On the other hand, however, SSG Reynolds stress, $k-\epsilon$, and $k-\epsilon$ RNG generally predict the lowest values, while the Spalart–Allmaras falls between both. An additional noticeable phenomenon is apparent in the mixing of the pressure side and suction side parts of the wakes, which differ between the models. In particular, the wake mixing with Spalart–Allmaras is greatly delayed when compared to other predictions. Even though the SSG Reynolds stress, $k-\epsilon$, and $k-\epsilon$ RNG have all been found to predict the lowest turbulent kinetic energy, the wake's strength appears to decay more slowly. Differences in modelling turbulence production and dissipation are believed to be the reason for this observation.

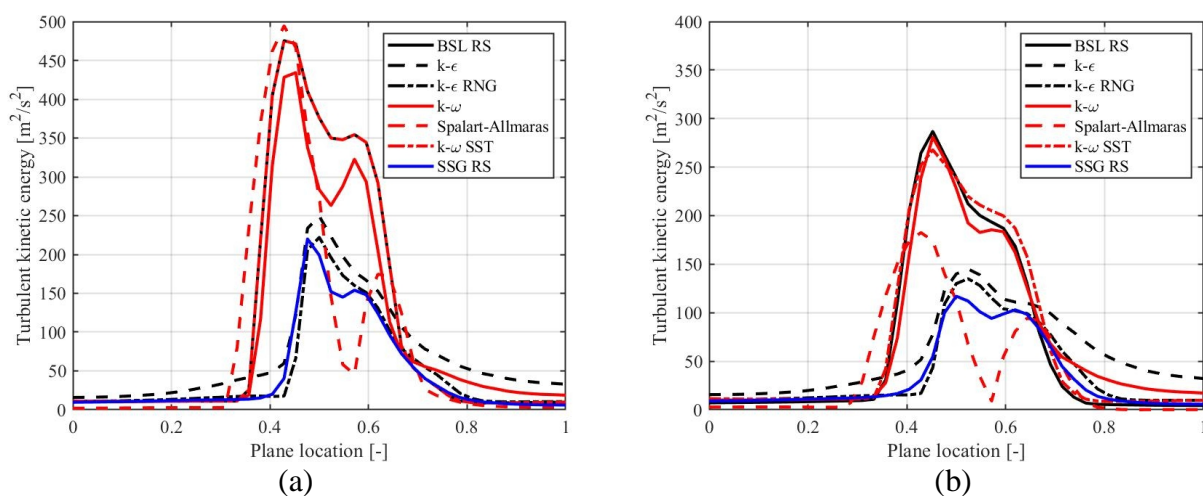


Figure 5: Effect of turbulence model on turbulent kinetic energy prediction at measurement plane 2 (a) and 3 (b).

CONCLUSIONS

This study first analysed the accuracy of Traupel's axial turbine loss model in the context of predicting primary losses in ROT cascades. Doing so showed that the model tends to over-predict profile loss when compared to all the seven turbulence models examined. This finding conforms well with previous studies focused on alternative axial turbine loss models.

The extent to which the turbulence modelling approach affects loss and fluid dynamic predictions was also analysed. The findings confirmed the approach to have a significant effect on results, with those noticeable differences concluded as mainly originating from the boundary layer and wake predictions, themselves made significant due to the variations in turbulence prediction capabilities of each model.

More specifically, it was found that Spalart–Allmaras turbulence models provide the highest accuracy to predict profile loss when compared to Traupel's model, followed by $k-\omega$ and $k-\omega$ SST. Similarly, when compared with the experimental isentropic Mach number distribution inside the blade channel, the three performance-wise best turbulence models were again found to be most accurate, together with the baseline Reynolds stress model. Regarding the accuracy of wake position prediction, $k-\omega$ and $k-\omega$ SST were the most accurate but very similar results were found with the Reynolds stress models and the Spalart–Allmaras model. When considering overall accuracy, it can be concluded that

both studied k - ε models agree least with the experimental data, as well as predicting pressure side flow acceleration phenomena near the trailing edge, which the best-performing models have not previously achieved. Furthermore, the results did not justify the computational efforts of Reynolds stress models since they did not provide improved prediction capability when compared to the best-performing two-equation and even the one-equation model.

As a final suggestion, either the k - ω or k - ω SST turbulence models should be used with radial outflow turbines. Spalart–Allmaras is also recommended as a third option. In future, it would also be beneficial to provide more validation data for ROTs, including different turbine vane and blade designs.

ACKNOWLEDGEMENTS

The authors would like to thank LUT University for providing funding to produce validation data.

REFERENCES

- Allmaras, S. R., Spalart, P. R. and Johnson, F. T., (2012). *Modifications and Clarifications for the Implementation of the Spalart–Allmaras Turbulence Model*. In Seventh International Conference on Computational Fluid Dynamics. Big Island, Hawaii.
- Al Jubori, A. M., Al-Dadah, R. K., Mahmoud, S., Daabo, A., (2017). *Modelling and parametric analysis of small-scale axial and radial-outflow turbines for organic rankine cycle applications*. Applied Energy, Vol. 190, pp. 981–996.
- Casati, E., Vitale, S., Pini, M., Persico, G., Colonna, P., (2014). *Centrifugal turbines for mini-organic Rankine cycle power systems*. Journal of Engineering for Gas Turbines and Power, Vol. 136, pp. 122607.
- Craig, H. R. M., Cox, H. J. A., (1971). *Performance estimation of axial flow turbines*. Proceedings of the Institution of Mechanical Engineers, Vol. 185, pp. 407–424.
- Dixon, S. L., (2005). *Fluid mechanics and thermodynamics of turbomachinery*. Fifth edition. Elsevier.
- Djouimaa, S., Messaoudi, L., Giel, P. W., (2007). *Transonic turbine blade loading calculations using different turbulence models – effects of reflecting and non-reflecting boundary conditions*. Applied Thermal Engineering, Vol. 27, pp.779–787.
- Grönman, A., Uusitalo, A., Backman, J., (2017). *Loss generation in radial outflow steam turbine cascades*. Proceedings of 12th European Conference on Turbomachinery Fluid Dynamics and Thermodynamics, April 3-7, Stockholm, Sweden, ETC2017-039.
- Grönman, A., Nerg, J., Sikanen, E., Sillanpää, T., Nevaranta, N., Scherman, E., Uusitalo, A., Uzhegov, N., Smirnov, A., Honkatukia, J., Sallinen, Jastrzebski, R. P., Heikkinen, J., Backman, J., Pyrhönen, J., Pyrhönen, O., Sopanen, J. and Turunen-Saaresti, T., (2020a). *Design and verification of a hermetic high-speed turbogenerator concept for biomass and waste heat recovery applications*. Energy Conversion and Management, Vol. 225, pp. 113427.
- Grönman, A., Tiainen, J., Uusitalo, A., (2020b). *Effects of Mach number and secondary flows on ultra-low aspect ratio radial outflow turbine cascade aerodynamics*. Proceedings of ASME Turbo Expo. GT2020-14146.
- Grönman, A. and Uusitalo, A., (2021). *Analysis of radial-outflow turbine design for supercritical CO₂ and comparison to radial-inflow turbines*. Energy Conversion and Management, Vol. 252, 115089.
- Kacker, S. C., Okapuu, U., (1981). *A mean line prediction method for axial flow turbine efficiency*. Journal of Engineering for Power, Vol. 104, pp. 111–119.

Launder, B. E. and Sharma, B. I., (1974). *Application of the energy-dissipation model of turbulence to the calculation of flow near a spinning disc*. Letters in Heat and Mass Transfer, Vol. 1, pp. 131-137.

Leino, M., Uusitalo, V., Grönman, A., Nerg, J., Horttanainen, M., Soukka, R., Pyrhönen, J., (2016). *Economics and greenhouse gas balance of distributed electricity production at sawmills using hermetic turbogenerator*. Renewable Energy, Vol. 88, pp. 102-111.

Lion S, Vlaskos I, Taccani R., (2020). *A review of emissions reduction technologies for low and medium speed marine Diesel engines and their potential for waste heat recovery*. Energy Conversion and Management, Vol. 207, pp. 112553.

Liu, Y., Yu, X., Liu, B., (2008). *Turbulence models assessment for large-scale tip vortices in an axial compressor rotor*. Journal of Propulsion and Power, Vol. 24, pp. 15-25.

Menter, F. R., (1993). *Zonal Two Equation $k-\omega$ Turbulence Models for Aerodynamic Flows*. In 24th AIAA Fluid Dynamics Conference, Orlando, Florida, AIAA Paper 93-2906.

Patel, Y., Turunen-Saaresti, T., Patel, G., Grönman, A., (2014). *Numerical Investigation of Turbulence Modelling on Condensing Steam Flows in Turbine Cascade*. Proceedings of ASME Turbo Expo, Düsseldorf, Germany, June 16-20, GT2014-26307.

Persico G, Pini M, Dossena V, Gaetani P., (2013). *Aerodynamic design and analysis of centrifugal turbine cascades*. Proceedings of ASME turbo expo, June 3-7, San Antonio, Texas, USA, GT2013-95770.

Pini M, Persico G, Casati E, Dossena V., (2013). *Preliminary design of a centrifugal turbine for organic Rankine cycle applications*. Journal of Engineering for Gas Turbines and Power, Vol. 135, pp. 042312.

Speziale, C. G., Sarkar, S. and Gatski, T. B., (1991). *Modelling the Pressure-strain Correlation of turbulence: an Invariant Dynamical Systems Approach*. Journal of Fluid Mechanics, Vol. 227, pp.245–272.

Traupel, W., (1977). *Thermische Turbomaschinen. Zweiter Band*. Springer-Verlag, Berlin-Heidelberg-New York.

Uusitalo, A., Nerg, J., Nikkanen, S., Grönman, A., (2019). *Numerical analysis on utilizing excess steam for electricity production in cruise ships*. Journal of Cleaner Production, Vol. 209, pp. 424-438.

Wilcox, D. C., (1994). *Turbulence modelling for CFD*. La Canada, California: Dcw Industries.

Yakhot, V., Orszag, S. A., Thangam, S., Gatski, T. B. and Speziale, C. G., (1992). *Development of turbulence models for shear flows by a double expansion technique*. Physics of Fluids A: Fluid Dynamics, Vol. 4, pp.1510–1520.

Yuan, Z., Zheng, Q., Yue, G., Jiang, Y., (2021). *Performance evaluation on radial turbines with potential working fluids for space closed Brayton cycle*. Energy Conversion and Management, Vol. 243, pp. 114368.

Zhdanov, I., Staudacher, S. and Falaleev, S., (2013). *An advanced usage of meanline loss systems for axial turbine design optimization*. Proceedings of ASME Turbo Expo, Turbine Technical Conference and Exposition, June 3-7, San Antonio, Texas, USA. GT2013-94323.